Anura3D
MPM Research Community

Paper number: mpm2019.05
www.anura3d.com
www.mpm2019.eu

Consistent Particle Method simulation of wave impact with air entrapment

Min Luo*
College of Engineering, Swansea University, UK SA1 8EN
* E-mail: min.luo@swansea.ac.uk

ABSTRACT

In this paper, the Consistent Particle Method (CPM) is introduced to model the wave impact with entrapped air pocket, in which the air compressibility matters. The novelty of CPM lies in three aspects: (1) accurate computation of Laplacian and gradient operators based on Taylor series expansion, (2) a thermodynamics-based compressible solver for modelling compressible air that eliminates the need of determining artificial sound speed, and (3) seamless coupling of the compressible air solver and incompressible water solver. The CPM model is used to simulate sloshing wave impact with entrapped air pocket in comparison with our experimental results.

KEY WORDS: Wave impact; air entrapment; particle method

INTRODUCTION

In many circumstances, violent fluid motions such as wave impacts on coastal/offshore structures generate air entrapment. The entrapped air may affect the amplitude and duration of impact pressure because of the air cushion effect. Substantial efforts have been devoted to this problem (Lind et al., 2015, Lind et al., 2017), but it is still not well understood. Simulation of this problem also remains a challenge. Particle methods offer a flexible alternative to mesh-based methods when simulating highly deformed water waves because of their meshless nature. In addition, by adopting a Lagrangian form of governing equation, particle methods can avoid the numerical dissipation induced by the discretization of the convection term in the governing equation.

Both the Smoothed Particle Hydrodynamics (SPH) and the Moving Particle Semi-implicit (MPS) are well-known particle methods, which use a kernel or weighting function to approximate the spatial derivatives by taking a weighted average based on particles within a given domain of influence. This strategy, however, can generate some numerical errors especially when the particle distribution is irregular (inevitable in violent fluid motion cases). Recently, a mathematically rigorous scheme based on Taylor series expansion was proposed to compute the gradient and Laplacian operators. This scheme was implemented into the framework of the incompressible SPH (or MPS). Because of the computation of the derivative satisfies the numerical consistency, this method was named the Consistent Particle Method (CPM) (Koh et al., 2012).

The main difficulties for CPM to simulate wave impact problems with air entrapment is the approximation of spatial derivatives with sharp density change and the integrated modelling of incompressible water and compressible air. To address these issues, an improvement of the derivative-approximation scheme in the single-phase CPM was recently proposed to deal with the sharp density discontinuity (Luo et al., 2015). In addition, a thermodynamically-consistent compressible solver that not only can be integrated with the developed incompressible solver seamlessly but also can overcome some issues encountered by other compressible solvers is developed (Luo et al., 2016). In this paper, the distinct features of CPM are presented systematically. The accuracy of CPM is demonstrated by an experimental study of sloshing wave impact with entrapped air pocket.

CPM METHODOLOGY

The governing equations of CPM are the Lagrangian Navier-Stokes equations, which are solved by the standard two-step projection method. More details are referred to Luo et al. (2016). The distinct features of CPM compared to other particle methods are introduced in the following sections.

Derivative computation based on Taylor series expansion

Based on Taylor series expansion, the first- and second-order derivatives are computed as follows:

$$\frac{\partial p_i}{\partial x} = \sum_j \left[w_j^2 \left(a_1 h_j + a_2 k_j + 0.5 a_3 h_j^2 + a_4 h_j k_j + 0.5 a_5 k_j^2 \right) \left(p_j - p_i \right) \right] = \sum_j \left[C_{1j} \left(p_j - p_i \right) \right] \quad (1)$$

$$\frac{\partial^2 p_i}{\partial x^2} = \sum_j \left[w_j^2 \left(c_1 h_j + c_2 k_j + 0.5 c_3 h_j^2 + c_4 h_j k_j + 0.5 c_5 k_j^2 \right) \left(p_j - p_i \right) \right] = \sum_j \left[C_{3j} \left(p_j - p_i \right) \right] \quad (2)$$

where w_j is a weighting function used in a weighted-least-square scheme (details are referred to Koh et al. (2012)), p_i and p_j the pressures on particles i and j respectively, and a and c the coefficients generated by the weighted-least-square scheme (refer to Equation (21) in Koh et al. (2012)). It should be noted that the weighting function in CPM formulations comes from the weighted-least-square solving scheme and is essentially different from the kernel function in SPH/ISPH and the weighting function in MPS.

Gradient and Laplace involving density discontinuity

In two-phase flows, the pressure is continuous at the fluid interface but its gradient changes drastically because of the large density difference between two fluids (e.g. water and air densities differ by three orders of magnitude) (Luo et al., 2015). Hence, when applied to pressure, the scheme introduced in the previous section does not give good approximation of gradient and Laplacian terms near the fluid interface. This problem, nevertheless, can be resolved by observing that the pressure gradient normalized with respect to density, i.e. $\nabla p / \rho$, is of the same order of magnitude in the two fluids of a general dynamic problem and, in the hydrostatic case, is in fact constant. By addressing the normalized pressure gradient term, the formulation to compute the gradient and Laplacian operators with abrupt density discontinuity can be derived (more details are given in Luo et al. (2015)):

$$\left(\frac{1}{\rho} \frac{\partial p}{\partial x} \right)_i = \sum_{j \neq i} \left[\frac{1}{0.5(\rho_i + \rho_j)} C_{1j} \left(p_j - p_i \right) \right] \quad (3) \qquad \left(\frac{\partial}{\partial x} \left(\frac{1}{\rho} \frac{\partial p}{\partial x} \right) \right)_i = \sum_{j \neq i} \left[\frac{1}{0.5(\rho_i + \rho_j)} C_{3j} \left(p_j - p_i \right) \right] \quad (4)$$

The coefficients C_{1j} and C_{3j} are the same as those in Equations (1) and (2) (Luo et al., 2015). The above reformulation retains the consistency with Taylor series expansion in computing the required gradient and Laplace terms with abrupt density discontinuity. This is a significant change and the first step in upgrading the single-phase CPM formulation to simulate two-phase flow problems. Note that in the single fluid domain far away from the interface (or in a single phase problem) where density discontinuity does not exist, Equations (3) and (4) revert to Equations (1) and (2). Thus the single-phase CPM is a special case of the two-phase formulation. Since no density smoothing or smearing scheme is needed, this scheme is able to model sharp fluid interfaces (e.g. water and air whose density difference is about three orders of magnitude) with good accuracy (Luo et al., 2015).

Compressible solver based on thermodynamics

For compressible flows, a closure condition is needed to solve the pressure Poisson equation (PPE). Selected to be the closure relation is the polytropic gas law $p/\rho^{\gamma} = \text{constant}$ (γ is the ratio of specific heats at constant pressure and constant volume and its value for air is about 1.4), since it does not require the input of speed of sound, which is dependent on the composition and temperature of a fluid. This avoids the need to determine the actual or numerical sound speed, in contrast to the c_s dependent equation of state (Luo et al., 2016).

In wave impact problems in marine and offshore engineering, there is little time for significant heat transfer to take place between an air pocket and the surrounding water particles (and solid boundary if any). Hence, it is reasonable to assume adiabatic conditions for air in wave impact problems. In addition, since the energy loss is small due to the low viscosity of air, the air expansion or compression process in two-phase flow problems can be approximated as reversible. With these two assumptions, the polytropic gas law with γ = 1.4 is applicable and will be utilized in the present study unless otherwise stated. This value has also been adopted in other numerical studies on wave impact problems (Zhang et al., 1996, Faltinsen et al., 2004) and verified experimentally by Abrahamsen and Faltinsen (2011) in their work of sloshing impact on tank walls.

Incorporating the polytropic gas law to the pressure equation, the PPE accounting for fluid compressibility can be derived as (Luo et al., 2016)

$$-\nabla \cdot \left(\frac{1}{\rho_i^*} \nabla p_i^{(k+1)} \right) + \frac{1}{\Delta t^2 \rho_i^*} \frac{\rho_{a0}}{p_{a0}} \frac{1}{\gamma} p_i^{(k+1)} = -\frac{1}{\Delta t^2} \frac{\rho_{a0} - \rho_i^*}{\rho_i^*} + \frac{1}{\Delta t^2 \rho_i^*} \frac{\rho_{a0}}{\gamma} \quad (5)$$

Since the speed of sound c_s is not involved in Equation (5), the issue of how to determine the actual value of c_s is avoided. This is a significant benefit of the present compressible solver. More importantly, this thermodynamically-consistent compressible solver and the solver for incompressible fluids both use the 2-step projection scheme to solve the same governing equations. The only difference lies in the treatment of fluid density in PPE. The compressible and incompressible solvers can thus be easily integrated, leading to the two-phase CPM model. It is capable of simulating two-phase incompressible and compressible flows with large density difference simultaneously. In addition, since the coefficient matrix of the PPE becomes better conditioned after bringing air compressibility in, the computational efficiency is improved and the spurious pressure fluctuation is further reduced (Luo et al., 2016). The accuracy of the 2-phase CPM model will be demonstrated by a benchmark example and an experimental study of wave impact with air entrapment, as elaborated in the following.

PERFORMANCE TEST IN HANDLING ABRUPT DENSITY DISCONTINUITY

The approximation of spatial derivatives near the fluid interface is challenging and of crucial importance for the simulation of two-phase flows. The capability of CPM to deal with this issue is demonstrated by the hydrostatic pressure distribution of a water-air two-phase flow system. For comparison purpose, the recently developed ISPH for multiphase flows (Zainali et al., 2013) is adopted here to model the same case. In both the CPM and ISPH simulations, the initial particle size of 0.01 m (1800 particles in total) and fixed time step of 0.001 s are used.

Figure 1 shows that the maximum normalized error (with respect to the analytical solution) of the simulated pressure by ISPH reaches about 90% near the fluid interface, while that of the CPM result is only about 3%. The inaccuracy in fluid pressure further leads to numerical error in the pressure gradient term. As shown in Figure 2, the normalized error of $\frac{1}{\rho}\frac{\partial p}{\partial y}$ (with respect to gravitational acceleration) in the ISPH result is more than twenty times larger than that in the CPM result. This shows the superior performance of the CPM in computing gradient and Laplacian operators with an abrupt density discontinuity at the fluid interface.

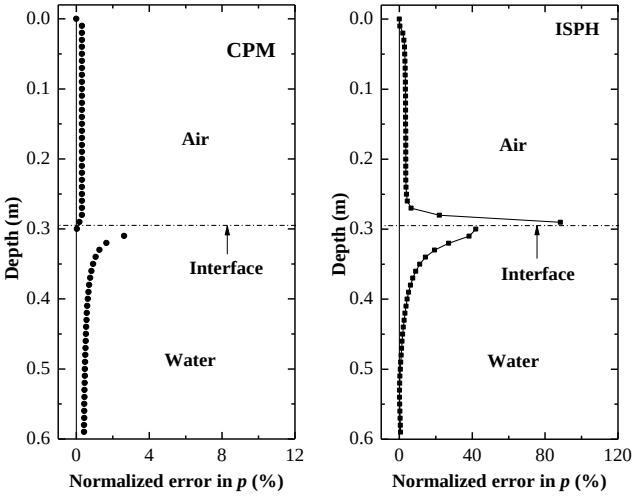

Figure 1 Normalized errors of simulated hydrostatic pressures by CPM and ISPH with respect to analytical solution

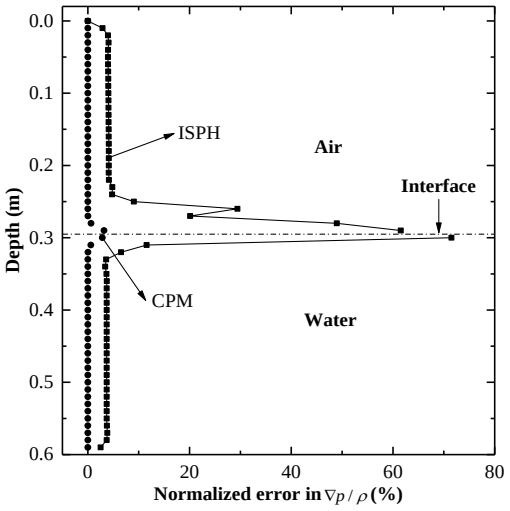

Figure 2 Normalized errors of simulated $\frac{1}{\rho}\frac{\partial p}{\partial y}$ by CPM and ISPH with respect to gravitational acceleration

SLOSHING IMPACT WITH ENTRAPPED AIR POCKET

Computational parameters

For validation purpose, a sloshing experiment is conducted in a specially designed container so that the shape and pressure variation of an air pocket can be measured (Luo et al., 2016). Figure 3 shows the overall setup of the sloshing experiments on a translational shake table. The water container comprises a big (left) tank connected by a short channel to a small (right) tank. It is designed such that when water in the left tank sloshes to the right (or left), some water will move through the connecting channel and compress (or expand) the air in the right tank. The air pressure at the middle of the top wall of the right tank, i.e. P_{A1} in Figure 4, is measured by an absolute pressure sensor. Water pressures at 60 mm from the bottom on the right wall of the right tank (P_{W1}), 145 mm from

the bottom on the right wall of the left tank (P_{W2}) and 30 mm from the bottom on the left wall of the left tank (P_{W3}) are measured by gauge pressure sensors. The translational motion of the shake table is measured by a displacement transducer and used as input for numerical simulations. The sloshing waves are recorded by a video camera at the front of the water container. The input displacement of the shake table is sinusoidal and governed by $x = -A(t)\cdot\sin(\omega t)$, where $A(t)$ is the amplitude of excitation and ω the excitation frequency. In order to avoid a sudden impulse on the fluid caused by non-zero initial velocity of the shake table, a ramping function of the excitation input is used as follows

$$A(t) = \begin{cases} A_0 t / t_r, & 0 \le t < t_r \\ A_0 \quad , & t \ge t_r \end{cases} \tag{6}$$

where t_r = 5s is the ramping time and A_0 = 0.0412 m the constant amplitude of excitation. Based on some preliminary studies, the filling depth is adopted to be 0.17 m (initial d_L and d_R in Figure 4) to have significant effect of the entrapped air pocket. The excitation frequency of $0.95\omega_0$ (= 3. 6807 rad/s) is found to generate a relatively large variation of air pressure in the right tank, where ω_0 is the reference frequency which is the natural frequency of water in the left tank only (ignoring the right tank) with water depth (d_L) and length (L_L) based on linear wave theory. In numerical simulation, an initial particle distance of 0.005 m (11,124 particles in total) and fixed time step 0.0005 s are adopted to achieve a good trade-off between accuracy and efficiency. The water and air densities at the NTP condition, i.e. 1000 kg/m^3 and 1.204 kg/m^3, as well as the initial air pressure of 1.01325×10^5 Pa are adopted. The dynamic viscosities of water and air are selected to be 10^{-3} Pa·s and 1.983×10^{-5} Pa·s respectively.

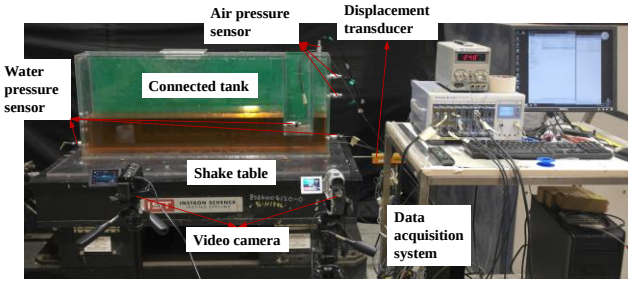

Figure 3 Water-air sloshing in a connected container under translational excitation

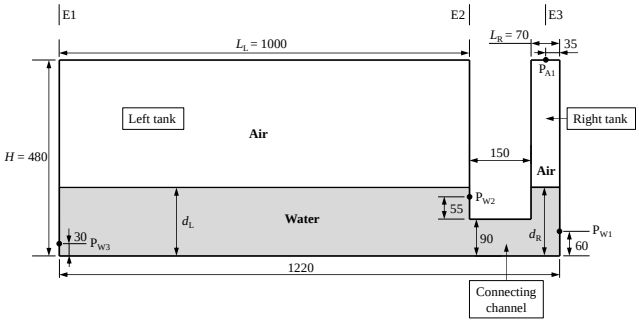

Figure 4 Geometric dimensions of the connected container used in sloshing experiments (Unit: mm)

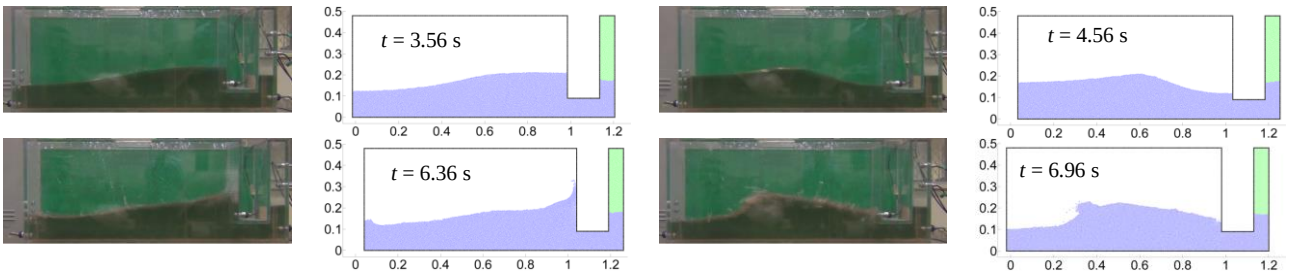

Figure 5 Wave profiles of sloshing with closed air pocket: experimental result and CPM simulation

Results and discussions

The numerical and experimental wave profiles at five time instants are compared in Figure 5, which shows generally good agreement. Because the filling level is low, the water in the left tank moves like a bore. This is consistent with the observation made by Wu et al. (1998). The bore becomes steeper and its amplitude becomes larger with time (see the snapshots at t = 3.56 s and 4.56 s in Figure 5). At t = 6.36 s (indicated by t_1 in Figure 6), the wave approaches the right side of the left tank and generates large impact force on the tank wall and water in the connecting channel (see Figure 6c). Consequently, water in the connecting channel is pushed towards right and compresses the enclosed air pocket in the right tank. As expected, a large peak of air pressure appears in the right tank, which is measured in the experiment and predicted well by CPM (Figure 6a). It is noteworthy that the amplitude of the air-pressure change is comparable to the dynamic pressure (gauge pressure minus the hydrostatic pressure) of the very violent and direct wave impact on the tank wall (see Figure 6c). However, even with such large pressure, the water level in the right tank changes only slightly relative to the initial water level. It means that even though air is compressible, the change of volume is small (unless a much larger force is applied). During

the impact process from t = 6.36 s to 6.96 s (t_2 in Figure 6), the air pressure in the right tank shows vibration. The mean air pressure at this stage is larger than the initial pressure because air is compressed. The air pressure also influences the water pressure near the air pocket (see the water pressure at Point P_{w1} as shown in Figure 6(b).

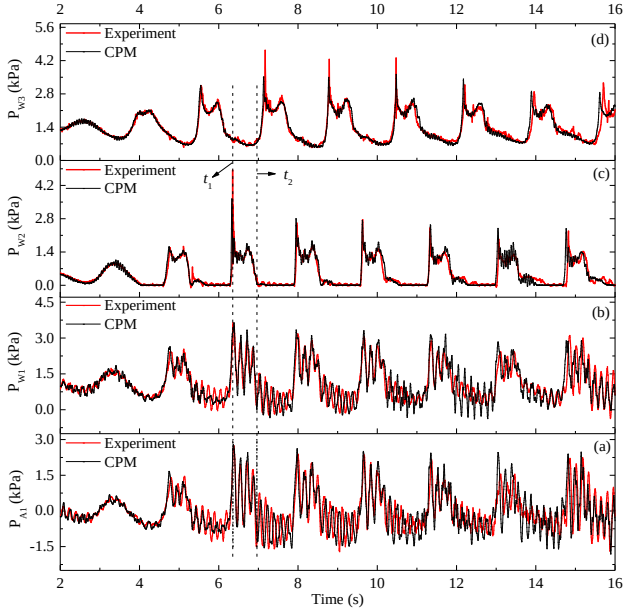

Figure 6. Simulated air pressure in comparison with experimental results

CONCLUSIONS

In this paper, the recently developed CPM is presented with distinct features in derivative computation and air compressibility modelling. By a benchmark example, the CPM is shown to reproduce the distributions of hydrostatic pressure and normalized pressure gradient near the water-air interface whose density difference is about three orders of magnitude. Using the validated CPM model, the sloshing wave impact with air entrapment is studied. An experimental study of water sloshing in a specially designed tank is conducted to measure the pressure change of a closed air pocket. Numerical results including wave profiles, sloshing pressures and particularly the pressure vibration in the air pocket predicted by CPM agree generally well with the experimental results.

ACKNOWLEDGEMENTS

The author appreciates the organizing committee of the conference.

REFERENCES

Abrahamsen, B. C. & Faltinsen, O. M. 2011. The effect of air leakage and heat exchange on the decay of entrapped air pocket slamming oscillations. *Physics of Fluids,* 23**,** 102107.

Faltinsen, O. M., Landrini, M. & Greco, M. 2004. Slamming in marine applications. *Journal of Engineering Mathematics,* 48**,** 187-217.

Koh, C. G., Gao, M. & Luo, C. 2012. A new particle method for simulation of incompressible free surface flow problems. *International Journal for Numerical Methods in Engineering,* 89**,** 1582–1604.

Lind, S., Fang, Q., Stansby, P., Rogers, B. D. & Fourtakas, G. 2017. Two-phase incompressible-compressible (water-air) smoothed particle hydrodynamics (ICSPH) method applied to focused wave slam on decks. *International Offshore and Polar Engineering Conference.* San Francisco , United States.

Lind, S. J., Stansby, P. K., Rogers, B. D. & Lloyd, P. M. 2015. Numerical predictions of water–air wave slam using incompressible–compressible smoothed particle hydrodynamics. *Applied Ocean Research,* 49**,** 57-71.

Luo, M., Koh, C. G., Bai, W. & Gao, M. 2016. A particle method for two-phase flows with compressible air pocket. *International Journal for Numerical Methods in Engineering,* 108**,** 695-721.

Luo, M., Koh, C. G., Gao, M. & Bai, W. 2015. A particle method for two-phase flows with large density difference. *International Journal for Numerical Methods in Engineering,* 103**,** 235-255.

Wu, G. X., Ma, Q. W. & Eatock Taylor, R. 1998. Numerical simulation of sloshing waves in a 3D tank based on a finite element method. *Applied Ocean Research,* 20**,** 337-355.

Zainali, A., Tofighi, N., Shadloo, M. S. & Yildiz, M. 2013. Numerical investigation of Newtonian and non-Newtonian multiphase flows using ISPH method. *Computer Methods in Applied Mechanics and Engineering,* 254**,** 99-113.

Zhang, S., Yue, D. K. P. & Tanizawa, K. 1996. Simulation of plunging wave impact on a vertical wall. *Journal of Fluid Mechanics,* 327**,** 221 - 254.